Calorimetry of amorphous calcium carbonate is correlated with its lithification and durability as synthetic stone—implications for CO$_2$ storage and utilization

Catherine Levey*, Jillian Reed [ID], Christopher Sanchez, Jacob Schneider and Brent R. Constantz

Blue Planet Systems Corporation, Los Gatos, CA, United States

The properties of amorphous calcium carbonate (ACC) and its transformations to crystalline polymorphs are frequently studied in aqueous systems and in small quantities. In this study, synthetic calcium carbonate stones are created from bulk ACC and crystalline polymorphs, which were precipitated from gaseous CO$_2$, at a gradient of end pH. Some of the ACCs hardened into stones which are durable against an abrasion and impact test, while some of the ACCs create fragile, friable stones. When ACCs which transform to durable stones and those which transform into fragile stones were subject to calorimetry, significant differences were observed. These stones, synthesized from gaseous CO$_2$, can be used as a storage reservoir for utilized CO$_2$ in construction and other infrastructure applications.

1 Introduction

The mineralization of CO$_2$ as solid stone is a permanent sequestration method for CO$_2$ emissions (Mazzotti et al., 2005). Most carbon on earth is in inorganic and mineral forms, particularly in carbonate rocks that contain a minimum of 40,000 times more carbon than in the atmosphere (Oelkers et al., 2008). Calcium carbonate, a carbonate mineral with the chemical name of limestone, is 44% CO$_2$ by weight and can be produced by a reaction of CO$_2$ with calcium hydroxide, Ca(OH)$_2$, also known as the mineral "portlandite" (Huntzinger et al., 2009).

Some scientists propose injecting waste CO$_2$ underground, where it can mineralize and be permanently stored (Mazzotti et al., 2005). The current study instead proposes utilizing the sequestered CO$_2$ by mineralizing it into calcium carbonate in a production facility and further processing it into hardened synthetic stones for use in construction. These synthetic calcium carbonate stones are chemically identical to limestone and could be used instead of natural limestone as aggregate in concrete. Concrete is the second most used material on earth after water, at approximately 30 billion tons per year (Monteiro et al., 2017). It is approximately 70% aggregate (sand and gravel-sized stones) by mass. Stones and sand, called "aggregate" in the industry, are also used for purposes such as asphalt; the total aggregate market is approximately 35 billion tons per year (O'Brien 2021). Therefore, if all construction

aggregate was replaced with synthetic stone which was 44% w/w mineralized CO_2, concrete and other construction aggregates could be a potential CO_2 storage reservoir for 15 billion tons of CO_2 per year. This upcycling CO_2 of construction materials can potentially store over a third of the 40 billion tons of CO_2 emitted into the atmosphere per year (Canadell et al., 2021).

Marine organisms mineralize strong structures in rapid timescales (Constantz, 1989; Constantz and Meike, 1989; Cartwright et al., 2012; Morse et al., 2007). We were inspired by nature to create biomimetic and geomimetic materials which sequester CO_2 at biological pHs in aqueous chemistry and rapidly biomineralize the CO_2 into strong materials, as do marine calcifying and aragonitic organisms. The learnings can be used both to study biomineralization using the methods described herein and to protect marine systems by capturing CO_2 emissions, thus preventing ocean acidification.

Calcium carbonate exists in three major crystal forms as well as in an amorphous phase. Under Ostwald's rule of stages, calcium carbonate precipitates as its less stable form, amorphous calcium carbonate (ACC), and then transforms to a meta-stable state, vaterite, and then to a stable state, either aragonite or calcite, depending on conditions (Bots et al., 2012).

It has been observed that ACCs formed under different conditions, whether chemical or biological, will transform into different polymorphs when they crystallize (Gebauer et al., 2010; Cartwright et al., 2012). Under synthetic conditions, some of the factors which can influence the crystallization of ACC include the presence of certain cations and anions such as magnesium, strontium, or sulfate, varying pH, and varying supersaturation (Bots et al., 2012; Jimoh et al., 2017; Albéric et al., 2018).

Various forms of ACC can be characterized by either structural methods, by their empirical properties, or by their transformation into the crystalline polymorphs of calcium carbonate (Shen et al., 2006; Albéric et al., 2018). This study examines the empirical properties of ACC *via* calorimetry and the ability of ACC to lithify or cement together into a durable synthetic stone during crystallization.

Tobler et al. (2016) found a link between the pH of the synthesis solution of calcium carbonate and the crystallization temperature of the resultant ACCs using calorimetry. Elsewhere, ACC transformation has been studied in the context of the transformation of the amorphous to the crystalline phase as a suspension or as a dispersed, finely-grained phase in an aqueous solution (Tobler et al., 2016; Bots et al., 2012; Albéric et al., 2018). These granular phases and their interactions can be simulated (Mergo and Seto, 2020). We build on these findings to study the link between the conditions of synthesis, the properties of ACC, and its transformation. The calcium carbonate is precipitated in bulk and shaped into synthetic stones. Some of the ACCs harden or lithify into durable stones, while others do not harden or lithify and are essentially a shaped powder. This study demonstrates, through defined processing and chemistries, that ACC can be made into consistent, load-bearing materials for sustainable building applications.

2 Methods and materials

2.1 ACC production

First, a calcium- and alkaline-rich solution was formed for the reactants to absorb CO_2 gas and form a $CaCO_3$ precipitate. To form this solution, a 1.5 M NH_4Cl solution was combined in a 1 kg solid: 1 kg liquid ratio with recycled crushed concrete containing portlandite—$Ca(OH)_2$. When the recycled concrete came into contact with the ammonium chloride solution, the following reaction occurred:

$$Ca(OH)_{2(s)} + 2NH_4Cl_{(aq)} -> CaCl_{2(aq)} + 2NH_{3(aq)} + 2H_2O_{(l)}$$
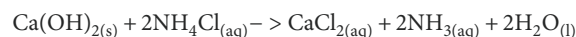
The concrete solids were then separated from the liquid, resulting in an aqueous solution with the calcium and alkalinity necessary to capture CO_2 as mineralized calcium carbonate—$CaCO_3$. The starting solution's pH was 9.13. Minor concentrations of additional ions were also present due to impurities in the raw material, which was an industrial waste product. The concentrations of the major constituents in the solution used were 298 mM Ca^{2+}, 1,506 mM Cl^-, 60 mM Na^+, 16 mM K^+, 227 mM NH_3, and 832 mM $NH4^+$.

A measure of 12 L of the pH 9.13 aqueous solution was poured into a 7-gallon (26.5 L) bucket used as a reactor, and 6% (w/w) CO_2 was pumped through a bubbling stone at 5 psi, 13 scfh, and an ambient temperature. As CO_2 was absorbed into the solution, the pH drop was monitored. At target pH values of 8.75, 8.50, 8.25, 8.00, 7.50, and 7.00, the CO_2 flow was paused, the solution was agitated to suspend the precipitate, and a representative aliquot was taken before the CO_2 flow was resumed on the bulk solution. For each aliquot, the sample was aged for 75 min to better represent internal bulk scale methods. At 75 min after sampling, each sample was filtered through a 1.5-μm filter paper and rinsed with five times its mass in tap water to remove the ammonium chloride. The samples at this stage were semisolids containing liquid water and the solid calcium carbonate precipitate, some of which was hydrous ACC containing chemically bound water. To stabilize the ACC, the liquid water needed to be removed such that only the calcium carbonate—including hydrous ACC—remained. Therefore, after rinsing the slurries with water, they were immediately (2 min or less) flash-frozen by submerging in liquid nitrogen. The flash frozen calcium carbonate samples were transferred to a lyophilizer until dry. Amorphous calcium carbonate has hygroscopic properties and can crystallize when it absorbs water from the air (Konrad et al., 2016), so the lyophilized samples were stored in a vacuum desiccator until measured. Konrad et al. (2016) demonstrated that ACC remains amorphous and that hydrous ACC retains its structural-bound water throughout lyophilization and storage in vacuum. Bates et al. (2013) have also shown that bound water can stay stable during and after lyophilization and that information about the bound water can be discerned during XRD analysis. The stability of the ACC and its hydration state through this process, including the aging step, was confirmed using our own ACC synthesis methods before beginning this experiment.

2.2 ACC measurement and analysis

Each lyophilized sample was measured on a Rigaku MiniFlex XRD system using Cu Kα radiation, from 15° to 90° 2θ, at a step size of 0.03° and a scan rate of 4° per minute.

Quantitative analysis of the XRD data was performed by the direct derivation analysis method on Rigaku's SmartLab Studio II software (Toraya 2018; Toraya 2021).

This method was developed by Toraya at Rigaku Corporation as a novel method of quantifying amorphous phases in XRD. It relies on a total diffraction pattern and the chemical formula of the amorphous phase to calculate the integrated contribution of each phase, including a known formula amorphous phase (Toraya 2016; Toraya 2018; Toraya 2021). See the cited literature for details on this method and its underlying theory.

The structural model of vaterite has been debated, and the nanocrystalline nature of vaterite creates barriers to classical single crystal diffraction studies (Burgess et al., 2014; Christy, 2017; Demichelis et al., 2013; Mugnaioli et al., 2012). The crystal structure most commonly used is hexagonal; however researchers have also proposed monoclinic, orthorhombic, and triclinic structures, as well as multiple point groups within each lattice system (Demichelis et al., 2013; Christy, 2017; Burgess et al., 2014).

The vaterite synthesized by the methods described here exhibits the major vaterite peaks and also diffracts a broad, asymmetric peak at 39° 2θ which is not found in the diffraction pattern of the hexagonal vaterite structure. The broad, asymmetric peak at 39° 2θ found in our diffraction pattern is described well by the triclinic structure model of Demichelis et al. (2013) or, more specifically, as a large number of small peaks between 38° and 41° 2θ. No single structure could describe our diffraction pattern alone, however, and we found that the best fit was a combination of the hexagonal (P63/mmc) and triclinic (C1) structure models, which was the same combination used by Demichelis et al. (2013) and Ševčík et al. (2015). Combinations of vaterite structures within single samples is described in the literature: Kabalah-Amitai et al. observed multiple crystallographic structures within a vaterite pseudo-single crystal, and Demichelis et al. proposed the rotation of carbonate ions within the superstructure at room temperature, resulting in room temperature interchange between symmetries. (Kabalah-Amitai et al., 2013; Demichelis et al., 2012; Demichelis et al., 2013).

Each lyophilized sample was measured for calorimetry on a Hitachi STA 7200 model from 30 C to 575 C at a 10 C/min ramp rate in aluminum pans with nitrogen flush.

For each sample, the peak temperature of each event was recorded, as well as the area under the peak (Figure 5A).

Replicates of $n = 7$ were run on one sample to determine the error of measurement of the TGA-x check graphs are determined by this sample.

2.3 Bulk synthetic stone preparation

Bulk samples were prepared separately from the preparation of the lyophilized samples and turned into synthetic stones to test the lithification of the precipitates and the resultant mechanical properties of the stones. The same aqueous solution from above

was purged with CO_2 using the same conditions. In four separate batches, the end pHs were pH 8.50, 8.00, 7.79, and 7.38. Each of these precipitates was aged to mimic production scale processing, filtered through a 1.5-µm filter paper; then the calcium carbonate filter cake was washed with five times its weight in tap water and filtered to a thick, semisolid consistency. This calcium carbonate and water mixture was shaped into approximately 0.5–2.5 cm rounded stones by tumbling in a rotating drum for approximately 10 min with heated air. These agglomerates cured over 7 days, of which the first 3 days were in a sealed bag.

2.4 Bulk synthetic stone measurement (durability test)

After the curing step, the stones were tested for durability (resistance to degradation by abrasion and impact) using a "mini Los Angeles (mini LA) abrasion test." This test is designed as a lab scale version of ASTM (American Society for Testing and Materials) test C131-06, a standard test for the aggregates industry whose title is "Standard Test Method for Resistance to Degradation of Small-Size Coarse Aggregate by Abrasion and Impact in the Los Angeles Machine" (ASTM, 2010). The mini LA abrasion test tumbles 15 g of the calcium carbonate stones with 1,500 g of steel balls (13 balls, three each at 1 1/2″, 1″, and 15/16″ and two at 7/8″) in a rotating cylinder with a shelf. The test tumbles for 1 min 45 s, after which the mass of calcium carbonate stones larger than a #12 (1.7 mm) mesh sieve are measured.

The result here is reported as the percentage surviving the test (g $CaCO_3$ which was larger than the sieve/g $CaCO_3$ initial), where more than 60% of the stones' mass surviving the test is a pass result in the ASTM test.
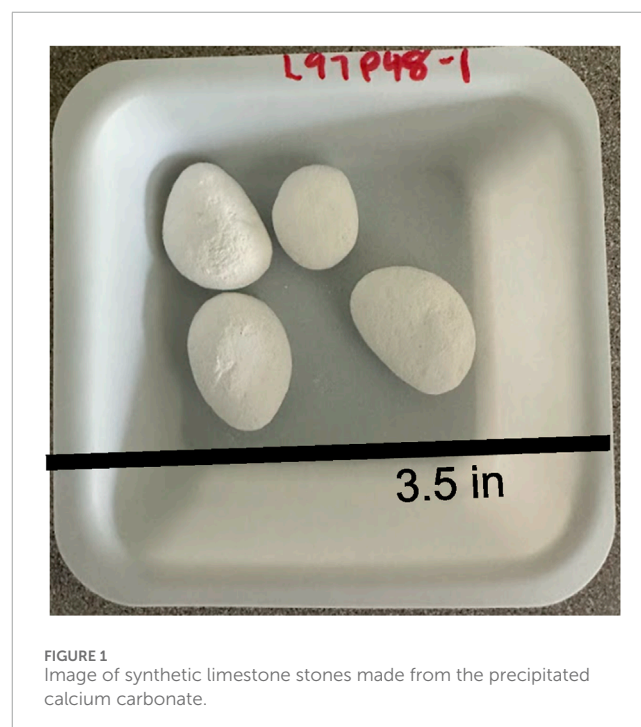

FIGURE 1
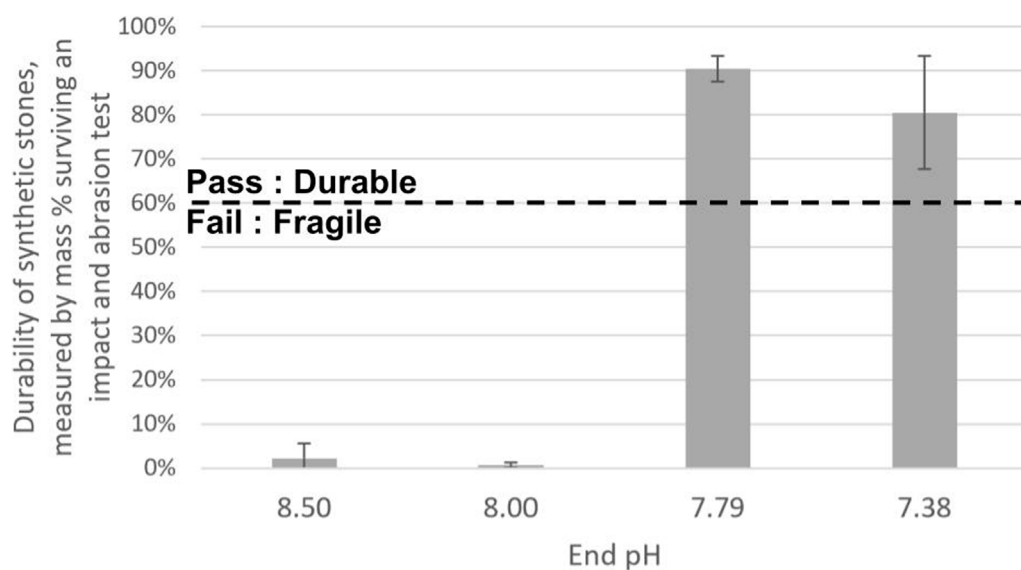Image of synthetic limestone stones made from the precipitated calcium carbonate.

FIGURE 2
Mass percentage which survived a durability (resistance to abrasion and impact) test. Calcium carbonate precipitated from a reaction which proceeded to an end pH below 8.00 produced bulk stones which survived the durability test (durable), while calcium carbonate precipitated from a reaction which was stopped at an end pH at or above 8.00 produced product which was degraded by the test (fragile).
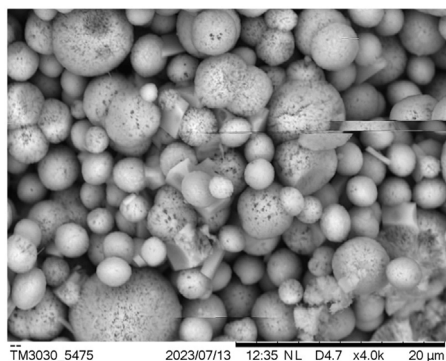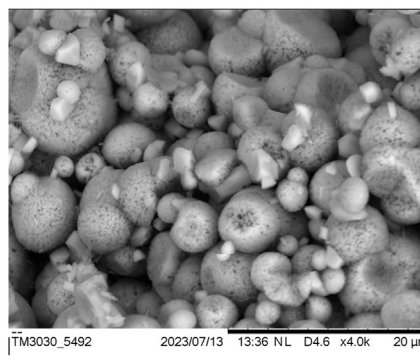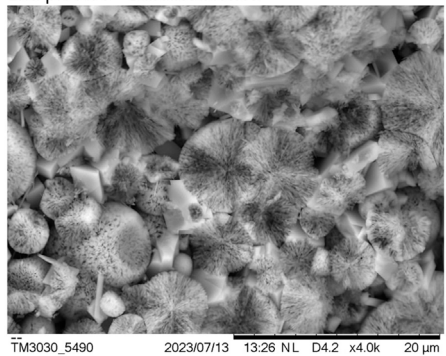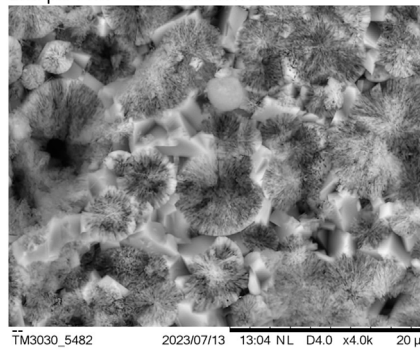

FIGURE 3
Microstructure of fracture surfaces of finished synthetic stones at a gradient of end pHs.
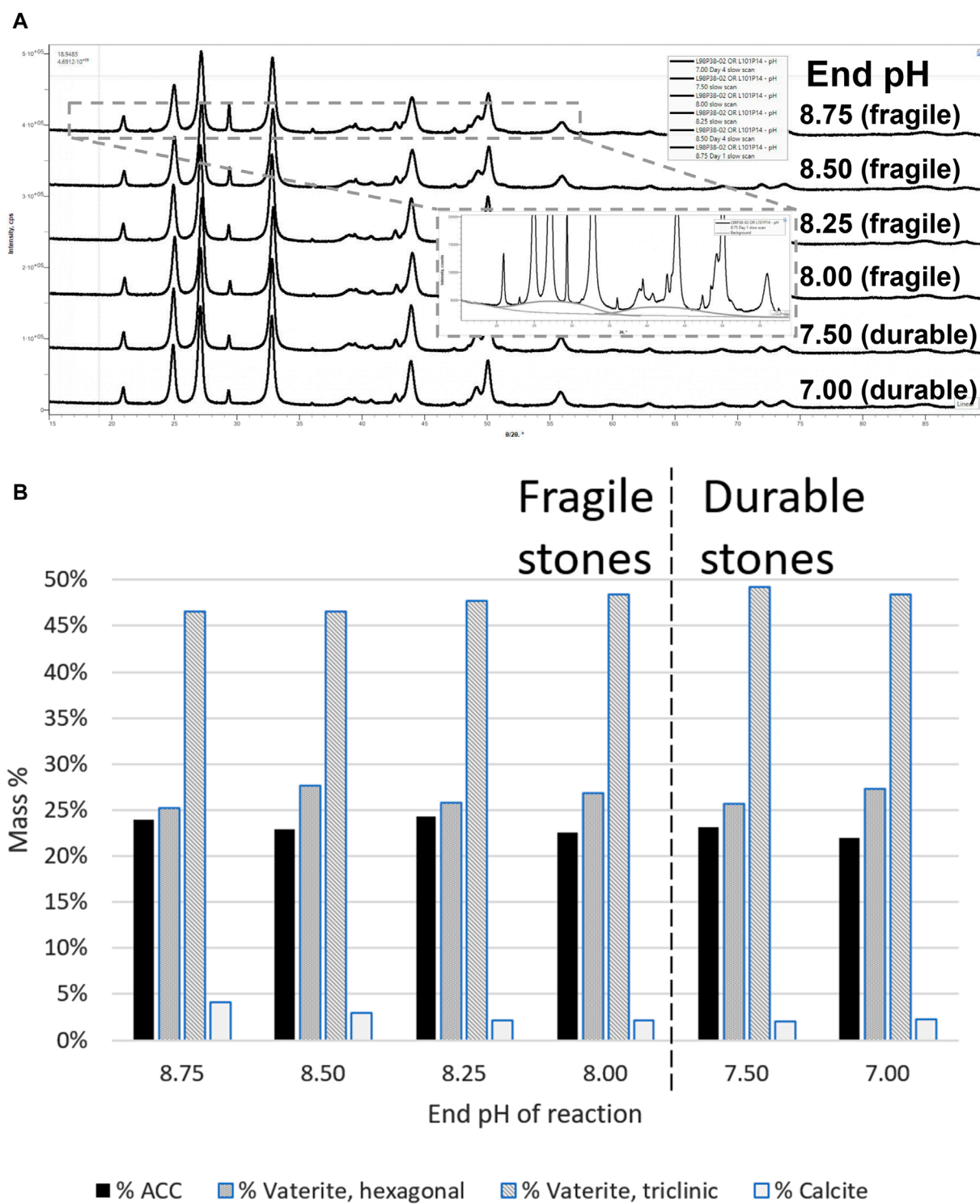
FIGURE 4
Polymorphic composition throughout the course of the reaction. **(A)** Raw XRD data and **(B)** quantitative phase analysis results.

A stone sample which passed the durability (resistance to degradation by abrasion and impact) test is referred to as "durable," while a stone sample which fails it is "fragile."

For imaging, each of the synthetic stones was cracked with a hammer, and the fracture surface imaged on SEM.

3 Results and discussion

3.1 Overview

The reactants for this CO_2 absorption and calcium carbonate utilization experiment were generated by extracting calcium and

alkalinity from waste concrete using an ammonium chloride solution. As gaseous CO_2 was absorbed, the pH dropped, and calcium carbonate precipitated. This precipitate was studied using XRD and calorimetry, and bulk precipitates were also prepared and shaped into synthetic stones.

The end pH had a dramatic correlation with the durability of the stones against abrasion and impact. Precipitate formed from a high-end pH of the reaction created friable, fragile stones, while reactions which proceeded further to a lower end pH created durable stones. The calcium carbonate precipitate which created friable and durable stones was comparable in polymorph composition, as quantified by XRD. However, when the precipitate was studied by calorimetry, differences were observed between the conditions, which resulted in fragile vs. durable stones. The precipitates which resulted in friable, fragile stones had two crystallization events and lower enthalpy release during each of the events. The precipitates which resulted in durable stones each had one crystallization event, which was more exothermic than either of the crystallization events in the fragile material precursors.

3.2 Synthetic stones and bulk properties

Synthetic stones from all reaction conditions had a rounded, oblong morphology, and the particle size was approximately 0.5–2.5 cm. Synthetic stones from all conditions were a pure white with a matte surface. Figure 1 shows an image of an aliquot of synthetic stones from the bulk precipitation reaction with end pH 7.38, which is representative of the centimeter-scale morphology of the stones from all reaction conditions.

Despite the similar appearances at the macro scale, the synthetic stones had widely varying durabilities. Some synthetic stones made from the bulk calcium carbonate precipitations survived the test for durability against abrasion and impact, while others were almost completely degraded. Figure 2 shows that, when the precipitation reaction from CO_2 capture was allowed to proceed to lower end pHs of 7.79 and 7.38, the stones were durable, with 80%–90% of their mass surviving the durability against abrasion and impact testing. However, when the precipitation reaction was stopped earlier at higher pHs of 8.50 and 8.00, the stones were highly fragile, defined by having less than 10% of their mass survive in the durability test.
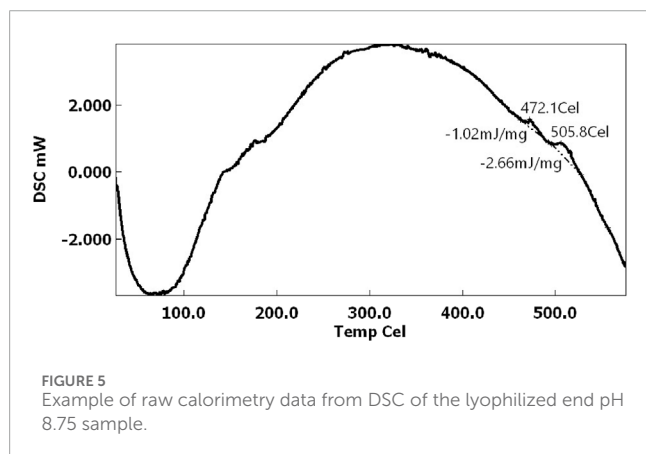

FIGURE 5
Example of raw calorimetry data from DSC of the lyophilized end pH 8.75 sample.

This wide range of durability led to an investigation of the microstructure and links between the microstructure of the cured or lithified stones and the observed durability properties. The structure–property relationship is apparent by observing the SEM images in Figure 3 of the fracture surfaces of the final synthetic stone products. The friable, fragile products form a packed calcium carbonate powder. As can be seen in Figures 3A, B, the first two samples are a packed powder of approximately 2–10 μm particles, with no interconnected structure between the precipitate particles. When a force is applied, the crack propagates between the particles, the calcium carbonate spheres become disconnected, and the product breaks down to a fine powder. In contrast, the durable products show a lithified, interconnected structure. The fracture propagates through the calcium carbonate spheres instead of between them. Therefore, the bonds between calcium carbonate particles are stronger than those within them because fractures propagate through the weakest points in a material. The durable sample in Figure 3D has a microstructure that appears as an inverse of the fragile and friable samples 3A and 3B. Since calcium carbonate transforms by dissolution–reprecipitation, the spaces between the spheres, which were previously the weak point of the structure, are now filled in with calcium carbonate, cementing into an interconnected continuous phase in the material, resulting in the integrity and cohesion of the durable samples.

In order to be used as construction materials, the stones must pass the ASTM C131-06 test—modified here to be a lab scale test we call the "durability against abrasion and impact test". Therefore, the stones that were synthesized with low-end pH reactions may be used in concrete, replacing mined virgin rocks such as limestone and providing a profitable market for captured CO_2.

3.3 Properties of calcium carbonate precipitate: XRD and calorimetry

The calcium carbonate precipitates from different reaction end pHs formed synthetic stones with widely varying properties and structures. In correlating precipitate to final synthetic stone properties, one hypothesis is that precipitate that forms fragile synthetic stone is different in polymorphic composition than precipitate that forms durable synthetic stone. For example, it could be that a higher ACC content in a precipitate leads to durable stones, and lower or no ACC content leads to fragile stones. To examine this, powder XRD was taken of each lyophilized sample.

The amounts of ACC, vaterite, and calcite stayed almost constant throughout the pH gradient (Figure 4). The XRD traces were quantified by the Direct Derivation quantiative analysis method, as discussed in the Methods Section 2.2. All differences are quantified to less than 3% (w/w absolute basis).

There was no apparent trend in ACC mass percentage throughout the pH range of the reaction. The ACC content was between 22.0% and 24.3% w/w for all samples. Because the quantity of ACC did not change significantly, the presumption is that one ACC type (lower temperature of crystallization) transformed into the other (higher temperature of crystallization). There were also no apparent trends in other polymorphs, except for calcite, which decreased from 4% to 2% over the first three samples (all of which result in fragile synthetic stones). When comparing the XRD results
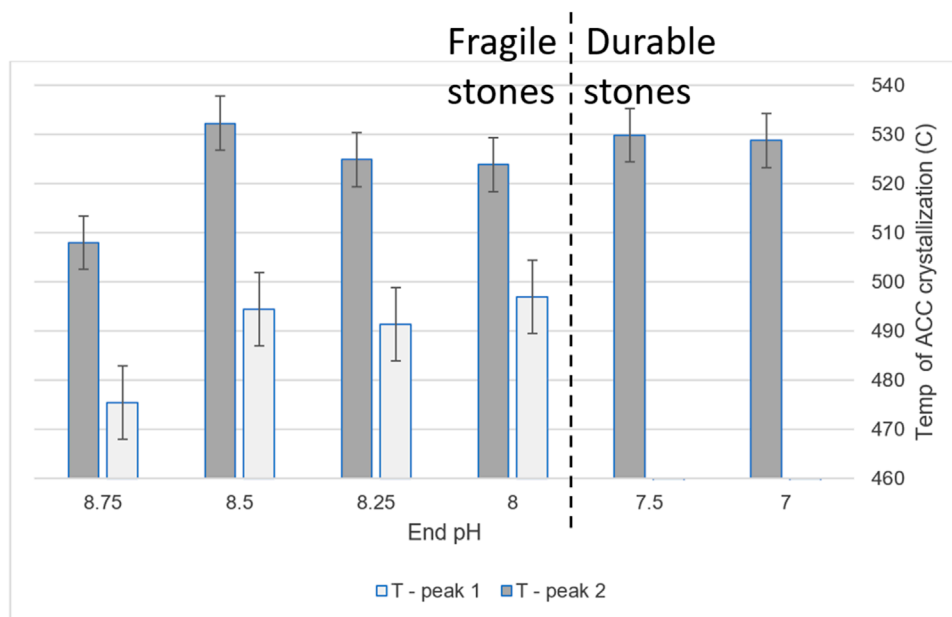
FIGURE 6
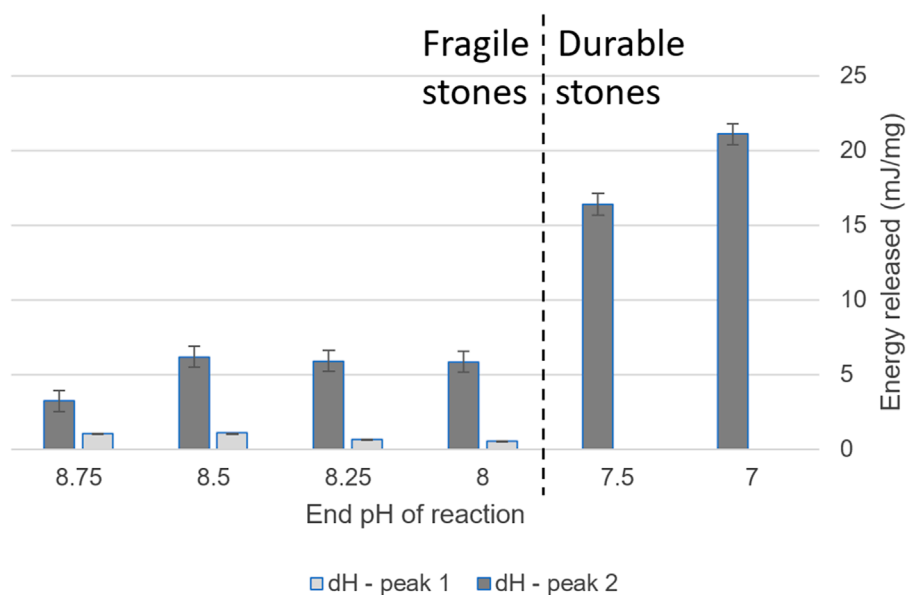Crystallization temperatures, as determined by DSC, of ACCs aliquoted throughout the pH gradient.

FIGURE 7
Enthalpy of ACC crystallization, as determined by DSC, of ACCs aliquoted throughout the pH gradient. All values are exothermic.

of the pH ranges that turn to fragile vs. durable synthetic stones, no significant difference was observed. Therefore, it can be concluded that the quantity of ACC or other polymorphs is not correlated with the calcium carbonate's ability to lithify to durable synthetic stone.

The next hypothesis examined was whether the ACC contained in the precipitates that lithify to durable synthetic stones is different from the ACC contained in the precipitates that form fragile stones. To assess the properties of these ACC materials, thermal calorimetry

was utilized to determine the exothermic character of the chemical transition from ACC to crystalline materials.

At the threshold between the fragile/failing and durable/passing range of the resultant stones, multiple changes were seen in the calorimetry of the ACCs.

The temperature of each exothermic peak was taken for each sample, as well as the area under the peak (Figure 5A). Figure 6 shows that the crystallization temperatures were replicable enough

to find statistically significant differences between the two major peaks (see *Methods and Materials* section). The data are shown with error bars from replicate measurements and analysis of the same sample.

The first significant change was in the number of crystallization events, or number of ACC types (Figure 6). Below pH 8.00, the range in which the precipitate transforms to durable stone, there was only one crystallization event instead of the two found at higher pHs, where the precipitate results in fragile stones. Samples with one type of ACC correlated with durable products, while slurries with two types of ACC correlated with fragile products. For both ACC types, there was also a significant increase in crystallization temperature between pH 8.75 to 8.50; however, this did not correspond to any observed difference in the resultant stones.

ΔH also correlated strongly with the resultant stone's durability (Figure 7). Crystallization became significantly more exothermic at the threshold of ACC that transformed to durable products. There are multiple possible causes for this increase in released energy during crystallization. Our hypotheses include the higher transition temperature ACC transforming to calcite instead of vaterite, or the ACC type being anhydrous, releasing less water. Another possible cause is that there was more of this type of ACC (that the energy released per mol was the same but the mass of this ACC phase was higher). The cause of the increase in exothermic nature is outside the scope of the current study. Future work should examine the cause of the difference in exothermic energy release, including characterization of the resultant crystalline phase(s). Future work could also investigate the effect of the lower crystallization temperature ACC on the transformation, such as a stabilizing effect that prevents dissolution–reprecipitation.

3.4 Conclusion

The present work utilizes techniques in ACC characterization and applies them in CO_2 capture, building materials, and structure–property relationships. The techniques and learnings may also be applied to biomineralization, where ACC's transformations to hardened materials are frequently studied. The calorimetry results of ACC are linked to its ability to lithify and form products. The end pH of the reaction can be selected to alter the CO_2 capture process to create the desired material properties from the same composition of calcium carbonate. Applying this fundamental research on ACC to creating synthetic stone could have a meaningful impact on climate change by allowing CO_2 to be utilized in building materials. Using the built environment as a reservoir for storing captured CO_2 can provide a commercial path to profitable and scalable CO_2 capture. In addition, biomineralogy research is interested in the crystallization of ACC into strong materials in shellfish. These mineralization processes in the marine environment have a pH near the threshold in the present study. Applying the results of the present study, especially the finding of an effect of pH on the durability of the materials, could be a fruitful path of research for biomineralization research.

Conflict of interest

Authors CL, JR, CS, JS, and BC were employed by Blue Planet Systems Corporation.

Publisher's note

References

Albéric, M., Bertinetti, L., Zou, Z., Fratzl, P., Habraken, W., and Politi, Y. (2018). The crystallization of amorphous calcium carbonate is kinetically governed by ion impurities and water. *Adv. Sci.* 5 (5), 1701000. doi:10.1002/advs.201701000

ASTM (2010). Standard test method for resistance to degradation of small-size Coarse aggregate by abrasion and impact in the Los Angeles machine. Available at: https://www.astm.org/standards/c131.

Bates, S., Jonaitis, D., and Nail, S. (2013). Sucrose lyophiles: a semi-quantitative study of residual water content by total X-ray diffraction analysis. *Eur. J. Pharm. Biopharm.* 85 (2), 184–188. doi:10.1016/j.ejpb.2013.05.011

Bots, P., Benning, L. G., Rodriguez-Blanco, J. D., Roncal-Herrero, T., and Shaw, S. (2012). Mechanistic insights into the crystallization of amorphous calcium carbonate (ACC). *Cryst. Growth & Des.* 12 (7), 3806–3814. doi:10.1021/cg300676b

Burgess, K. M., and Bryce, D. L. (2014). On the crystal structure of the vaterite polymorph of CaCO3: a calcium-43 solid-state NMR and computational assessment. *Solid State Nuclear Magnetic Resonance* 65, 75–83.

Canadell, J. G., Monteiro, P. M., Costa, M. H., Da Cunha, L. C., Cox, P. M., Eliseev, A. V., et al. (2021). *Global carbon and other biogeochemical cycles and feedbacks.*

Cartwright, J. H., Checa, A. G., Gale, J. D., Gebauer, D., and Sainz-Díaz, C. I. (2012). Calcium carbonate polyamorphism and its role in biomineralization: how many amorphous calcium carbonates are there? *Angew. Chem. Int. Ed.* 51 (48), 11960–11970. doi:10.1002/anie.201203125

Christy, A. G. (2017). A review of the structures of vaterite: the impossible, the possible, and the likely. *Crystal Growth and Design* 17 (6), 3567–3578.

Constantz, B., and Meike, A. (1989). "Calcite centers of calcification in Mussa angulosa (Scleractinia)," in *Origin, evolution, and modern aspects of biomineralization in plants and animals* (Boston, MA: Springer US), 201–207.

Constantz, B. R. (1989). "Skeletal organization in caribbean Acropora spp.(Lamarck)," in *Origin, evolution, and modern aspects of biomineralization in plants and animals* (Boston, MA: Springer US), 175–199.

Demichelis, R., Raiteri, P., Gale, J. D., and Dovesi, R. (2012). A new structural model for disorder in vaterite from first-principles calculations. *CrystEngComm* 14 (1), 44–47. doi:10.1039/c1ce05976a

Demichelis, R., Raiteri, P., Gale, J. D., and Dovesi, R. (2013). The multiple structures of vaterite. *Cryst. growth & Des.* 13 (6), 2247–2251. doi:10.1021/cg4002972

Gebauer, D., Gunawidjaja, P. N., Ko, J. P., Bacsik, Z., Aziz, B., Liu, L., et al. (2010). Proto-calcite and proto-vaterite in amorphous calcium carbonates. *Angew. Chem. Int. Ed.* 49 (47), 8889–8891. doi:10.1002/anie.201003220

Huntzinger, D. N., Gierke, J. S., Kawatra, S. K., Eisele, T. C., and Sutter, L. L. (2009). Carbon dioxide sequestration in cement kiln dust through mineral carbonation. *Environ. Sci. Technol.* 43 (6), 1986–1992. doi:10.1021/es802910z

Jimoh, O. A., Ariffin, K. S., Hussin, H. B., and Temitope, A. E. (2017). Synthesis of precipitated calcium carbonate: a review. *Carbonates Evaporites* 33 (2), 331–346. doi:10.1007/s13146-017-0341-x

Kabalah-Amitai, L., Mayzel, B., Kauffmann, Y., Fitch, A. N., Bloch, L., Gilbert, P. U., and Pokroy, B. (2013). Vaterite crystals contain two interspersed crystal structures. *Science* 340 (6131), 454–457.

Konrad, F., Gallien, F., Gerard, D. E., and Dietzel, M. (2016). Transformation of amorphous calcium carbonate in air. *Cryst. growth & Des.* 16 (11), 6310–6317. doi:10.1021/acs.cgd.6b00906

Mazzotti, M., Abanades, J. C., Allam, R., Lackner, K. S., Meunier, F., Rubin, E., et al. (2005). "Mineral carbonation and industrial uses of carbon dioxide," in *IPCC special report on carbon dioxide capture and storage* (Cambridge: Cambridge University Press), 330. section 7.2.8.1.

Mergo, J., and Seto, J. (2020). On simulating the formation of structured, crystalline systems via non-classical pathways, *Front. Mater* 7. 75. doi:10.3389/fmats.2020.00075

Monteiro, P. J., Miller, S. A., and Horvath, A. (2017). Towards sustainable concrete. *Nat. Mater.* 16 (7), 698–699. doi:10.1038/nmat4930

Morse, J. W., Arvidson, R. S., and Lüttge, A. (2007). Calcium carbonate formation and dissolution. *Chem. Rev.* 107 (2), 342–381. doi:10.1021/cr050358j

Mugnaioli, E., Andrusenko, I., Schüler, A., Loges, N., Dinnebier, R. E., Panthöfer, M., et al. (2012). Ab initio structure determination of vaterite by automated electron diffraction. *Angewandte Chemie International Edition* 51 (28), 7041–7045.

O'Brien, J. (2021). Growing global aggregates sustainably. Aggregates Business. Available at: https://www.aggbusiness.com/feature/growing-global-aggregates-sustainably (Accessed December 22, 2023).

Oelkers, E. H., Gislason, S. R., and Matter, J. (2008). Mineral carbonation of CO2. *Elements* 4 (5), 333–337. doi:10.2113/gselements.4.5.333

Ševčík, R., Pérez-Estébanez, M., Viani, A., Šašek, P., and Mácová, P. (2015). Characterization of vaterite synthesized at various temperatures and stirring velocities without use of additives. *Powder Technol.* 284, 265–271. doi:10.1016/j.powtec.2015.06.064

Shen, Q., Wei, H., Zhou, Y., Huang, Y., Yang, H., Wang, D., et al. (2006). Properties of amorphous calcium carbonate and the template action of vaterite spheres. *J. Phys. Chem. B* 110 (7), 2994–3000. doi:10.1021/jp055063o

Tobler, D. J., Rodriguez Blanco, J. D., Sørensen, H. O., Stipp, S. L., and Dideriksen, K. (2016). Effect of pH on amorphous calcium carbonate structure and transformation. *Cryst. Growth & Des.* 16 (8), 4500–4508. doi:10.1021/acs.cgd.6b00630

Toraya, H. (2016). A new method for quantitative phase analysis using X-ray powder diffraction: direct derivation of weight fractions from observed integrated intensities and chemical compositions of individual phases. *J. Appl. Crystallogr.* 49 (5), 1508–1516. doi:10.1107/s1600576716010451

Toraya, H. (2018). Direct derivation (DD) of weight fractions of individual crystalline phases from observed intensities and chemical composition data: incorporation of the DD method into the whole-powder-pattern fitting procedure. *J. Appl. Crystallogr.* 51 (2), 446–455. doi:10.1107/s1600576718001474

Toraya, H. (2021). Review of the direct derivation method: quantitative phase analysis with observed intensities and chemical composition data. *Powder Diffr.* 36 (3), 159–168. doi:10.1017/s0885715621000373